1676–1685 *Nucleic Acids Research, 2010, Vol. 38, No. 5* *Published online 8 December 2009*
doi:10.1093/nar/gkp1107

An intermolecular RNA triplex provides insight into structural determinants for the pseudoknot stimulator of −1 ribosomal frameshifting

Ming-Yuan Chou and Kung-Yao Chang*

Graduate Institute of Biochemistry, National Chung-Hsing University, 250 Kuo-Kung Road, Taichung 402, Taiwan

Received June 16, 2009; Revised November 8, 2009; Accepted November 10, 2009

ABSTRACT

An efficient −1 programmed ribosomal frameshifting (PRF) signal requires an RNA slippery sequence and a downstream RNA stimulator, and the hairpin-type pseudoknot is the most common stimulator. However, a pseudoknot is not sufficient to promote −1 PRF. hTPK-DU177, a pseudoknot derived from human telomerase RNA, shares structural similarities with several −1 PRF pseudoknots and is used to dissect the roles of distinct structural features in the stimulator of −1 PRF. Structure-based mutagenesis on hTPK-DU177 reveals that the −1 PRF efficiency of this stimulator can be modulated by sequential removal of base–triple interactions surrounding the helical junction. Further analysis of the junction-flanking base triples indicates that specific stem–loop interactions and their relative positions to the helical junction play crucial roles for the −1 PRF activity of this pseudoknot. Intriguingly, a bimolecular pseudoknot approach based on hTPK-DU177 reveals that continuing triplex structure spanning the helical junction, lacking one of the loop-closure features embedded in pseudoknot topology, can stimulate −1 PRF. Therefore, the triplex structure is an essential determinant for the DU177 pseudoknot to stimulate −1 PRF. Furthermore, it suggests that −1 PRF, induced by an in-trans RNA via specific base–triple interactions with messenger RNAs, can be a plausible regulatory function for non-coding RNAs.

INTRODUCTION

During translation, the ribosomes have to maintain correct reading frame to faithfully decode the in-frame messenger RNA (mRNA) sequences into ordered amino acid sequences. However, specific information within mRNAs can trigger the slippage of reading frames for elongating ribosomes, and thus lead to the frameshifting events (1). In one case, the ribosomes are induced to move backward one base in the 5′ direction in response to specific signals within mRNAs, and then continue translation in the new −1 reading frame (2). Such a −1 programmed ribosomal frameshifting (PRF) is adopted by a variety of viruses to maintain a specific ratio between structural and enzymatic proteins (3–7), and examples of −1 PRF in cellular genes are also reported (8–10). The mechanism for the induction of −1 PRF by a stimulator is a delicate process and may involve multiple factors. Efficient eukaryotic −1 PRF requires two in *cis* RNA elements within the mRNA (11,12): a heptanucleotide slippery site of XXXYYYZ sequences, where the frameshift occurs, and a downstream RNA structure connected by a spacer. The optimal distance between stimulator and slippery site, separated by the spacer, will then position the A- and P-site tRNAs on the slippery site (13–15). With the sequence feature of X being any three identical nucleotides, Y being either AAA or UUU, and Z not being a G, these cooperative RNA elements can increase the probability of a ribosome to slip with A- and P-site tRNAs in the 5′ direction by one base along the mRNA (from X XXY YYZ to XXX YYY Z) (15).

The downstream RNA stimulator is usually a hairpin-type RNA pseudoknot in which nucleotides from a hairpin loop form base pairs with a single-stranded region outside the hairpin. It leads to a quasi-continuous RNA double-helical structure, with a topology featuring two helical stems of the base-pairing region (stems 1 and 2) connected by two single-stranded loops (loops 1 and 2) (16). It is thought that the resistance of a stimulator against deformation by the ribosome helicase activity can cause the marching ribosome to pause. However, RNA hairpin not capable of stimulating −1 PRF also causes the ribosome to pause (13,14,17). As unwinding of stem 1 by ribosome will require rotation of the rest of the pesudoknot, torsional restraint hypothesis suggests that pseudoknot topology can restrain loop rotation during

*To whom correspondence should be addressed. Tel: +886 4 22840468 (ext. 218); Fax: +886 4 22853487; Email: kychang@dragon.nchu.edu.tw

the unwinding of stem 1, and thus interferes with this process (18). Interestingly, only a subset of RNA pseudoknots can stimulate −1 PRF and non-pseudoknot RNA elements have been characterized to induce −1 PRF (19–21), implicating the existence of uncharacterized determinants. In addition, the involvement of specific interactions between pseudoknot stimulator and ribosomal components during the unwinding process cannot be ruled out (22,23).

Based on the length of stem 1, the RNA pseudoknots capable of stimulating −1 PRF can be classified into two groups. One group of pseudoknot requires a long stem 1 to stimulate −1 PRF efficiently and can be represented by the infectious bronchitis virus pseudoknot (IBV-PK), which contains 11 bp in stem 1. Deviation from the optimal 11–12 bp in stem 1 will lead to the impairment of IBV-PK frameshift efficiency (24). However, no high-resolution structural information is available for this class of pseudoknot. In contrast, the other group of pseudoknots, which includes mouse mammary tumor virus pseudoknot (MMTV-PK), beet western yellow virus (BWYV-PK) and simian retrovirus pseudoknot (SRV-PK), has a short stem 1 of <7 bp in length (16). The analysis of high-resolution structures of several short stem 1 possessing pseudoknots indicated that they all share a common structural feature, involving tertiary loop-helix interactions (between stem 1 and loop 2) close to the helical junction (22,25–28). The requirement of these tertiary interactions in −1 PRF activity has been verified by mutagenesis analysis (29–32). However, the relative small size of this group of pseudoknots makes it difficult to rationalize the results of extensive mutagenesis analysis because a mutant may not necessarily still form a pseudoknot. Furthermore, NMR structures of a luteoviral pseudoknot and its poorly functional variant suggest that both pseudoknots possess essentially identical global structure (27,28). Therefore, how structurally similar pseudoknots produce distinct −1 PRF efficiency remains an open question.

Here, we demonstrate that an RNA pseudoknot, hTPK-DU177 (DU177), which is derived from human telomerase RNA (33,34), can function as an efficient −1 PRF stimulator. Because well-characterized −1 PRF pseudoknots containing short stem 1 all possess relative short loop 1 (22,25–28), information for the contribution of loop 1–stem 2 interactions to −1 PRF activity of a pseudoknot is limited (18). Therefore, the long loop 1 of DU177 and its extensive stem–loop interactions with the stem 2 make this well-defined pseudoknot an excellent model to explore this issue. Using DU177 and its variants, we show that the −1 PRF efficiency of DU177 can be impaired by the disruption of specific base–triple interactions flanking the helical junction region. In contrast, a DU177 mutant, lacking most of the triple interactions identified in DU177, has essentially no frameshift activity but still adopts a pseudoknot conformation. Furthermore, the triplex in DU177 is then mimicked and constructed intermolecularly (35), and is used to decouple triplex formation from pseudoknot topology to resolve their roles in −1 PRF activity. Therefore, our work provides a platform to characterize the contributions of two structural determinants of a −1 PRF pseudoknot. Finally, the results from this work also imply that a non-coding RNA may act in-trans to stimulate −1 PRF on targeted mRNAs by specific intermolecular triplex formation.

MATERIALS AND METHODS

Construction of reporter genes and mutagenesis

The p2luc reporter was a kind gift from Professor John Atkins at the University of Utah (36), and the pRL-SV40 vector was purchased from Promega. Oligonucleotides containing the slippery sequence (TTTAAAC), spacer (GGGTT) and the stimulator sequences were chemically synthesized. They were amplified by forward and reverse primers containing *BsrG*I and *BsaA*I sites, respectively, and ligated into the *BsrG*I/*BsaA*I sites (1392/1426) of pRL-SV40 vectors treated with restriction enzymes. Oligonucleotides containing DU177, hTR-5′hp, hTR5′hp-L1c and hTR174T5′hp sequences were also inserted into p2luc reporter in a similar way, except for the use of *Sal*I and *BamH*I restriction sites instead. A −1-frame stop codon was inserted into the DU177-containing p2luc reporter, thus generating a premature −1-frame protein product, to facilitate the −1 PRF assays of DU177-related variants *in vitro* (37). All of the mutants were constructed using the quick-change mutagenesis kit from Stratgene, and the identities of all cloned and mutated genes were confirmed by DNA sequencing analysis.

RNA synthesis and enzymatic structure probing

RNA transcripts were generated by *in vitro* transcription using T7 RNA polymerase. The purified RNAs of desired length were then dephosphorylated by calf intestine alkaline phosphatase, 5′-end labeled with [γ-^{32}P] ATP using T4 polynucleotide kinase, and then separated by a 20% sequencing gel for recovery. All the RNase protection experiments were performed with 50 000 to 70 000 cpm of 5′-end labeled RNA in the presence of RNase cleavage buffer (30 mM Tris-HCl, pH 7.5; 3 mM EDTA; and 100 mM LiCl) for each reaction, and 10 mM $MgCl_2$ were included in the same buffer for RNase V1 experiments. Before the addition of probing enzymes, the RNAs were denatured by heating at 65°C for 5 min and followed by slow cooling to 20°C for structural mapping. Finally, 0.02–0.5 U of RNase T2 (USB) or 0.02–0.5 U of RNase V1 (Amersham Pharmacia) was added to each reaction. The hydrolysis RNA ladders were obtained by incubation of RNA in the hydrolysis buffer at 100°C for 2 min, and parallel RNA sequencing products were obtained by the treatment of unfolded RNA with RNases T1 or A. They were used as markers for the assignment of guanines and pyrimidines, respectively. All reactions were incubated at 20°C for 10 min unless specified. The reactions were terminated by addition of gel loading dye, and the cleavage products were resolved by a 20% denaturing gel and visualized by phosphorimagery.

Gel mobility assay by non-denatured gel electrophoresis

The purified RNAs were analyzed on a 20% non-denatured polyacrylamide gel (29:1 acryl:bisacryl ratio) in the 1× TBE (Tris-Borate-EDTA) buffer. The gel was run at a constant voltage of 150 V for 8 h at room temperature. The results were visualized by the staining of ethidium bromide.

In vitro translation and −1 PRF assay

The capped reporter mRNAs were prepared by the mMESSAGE mMACHINE high-yield capped RNA transcription kit (Ambion) by following the manufacturer's instructions. The reticulocyte lysate system (Progema) was used to generate the shifted and non-shifted protein products. In each assay, a total of 5 µl reaction containing 250 ng of capped reporter mRNA, 2.5 µl of reticulocyte lysate and 0.2 µl of 10 µCi/µl ^{35}S-labeled methionine (NEN) was incubated at 30°C for 1.5 h. The samples were then resolved by 12% SDS polyacrylamide gels and exposed to phosphorimager screen for quantification after drying. The −1 PRF efficiency was calculated by dividing the counts of the shifted product by the sum of the counts for both shifted and non-shifted products, with calibration of the methionine residue number in each product.

RESULTS

Both major-groove and minor-groove triple interactions are required for the −1 PRF activity of DU177

A comparison between DU177 and several representative −1 PRF pseudoknot stimulators (Figure 1A–F) revealed a consensus AACAA sequence in the loop 2 of three short stem 1-containing pseudoknots (Figure 1C–E). Furthermore, both PEMV-1 PK and DU177 contain an unusual Hoogsteen AU base pair, formed between loops 1 and 2, to bridge the helical junction. We thus examined if DU177 could function as a −1 PRF stimulator when it is positioned downstream of a slippery sequence. To this end, the −1 PRF activity of DU177 was measured and compared with those of several well-characterized pseudoknot stimulators available in our laboratory. The results, shown in Figure 1G, indicate that DU177 can act as an efficient −1 PRF stimulator *in vitro*. The −1 PRF efficiency stimulated by DU177 was comparable with that of the minimal IBV pseudoknot (IBVm-PK) and was in the range of 50%. This value was higher than those of MMTV-PK (24%) and the other two AACAA-containing pseudoknots, BWYV-PK and SRV-PK (21% and 34%, respectively). In addition, DU177 possessed substantial −1 PRF activity *in vivo* (data not shown). Therefore, the high −1 PRF activity and the well-resolved structure of DU177

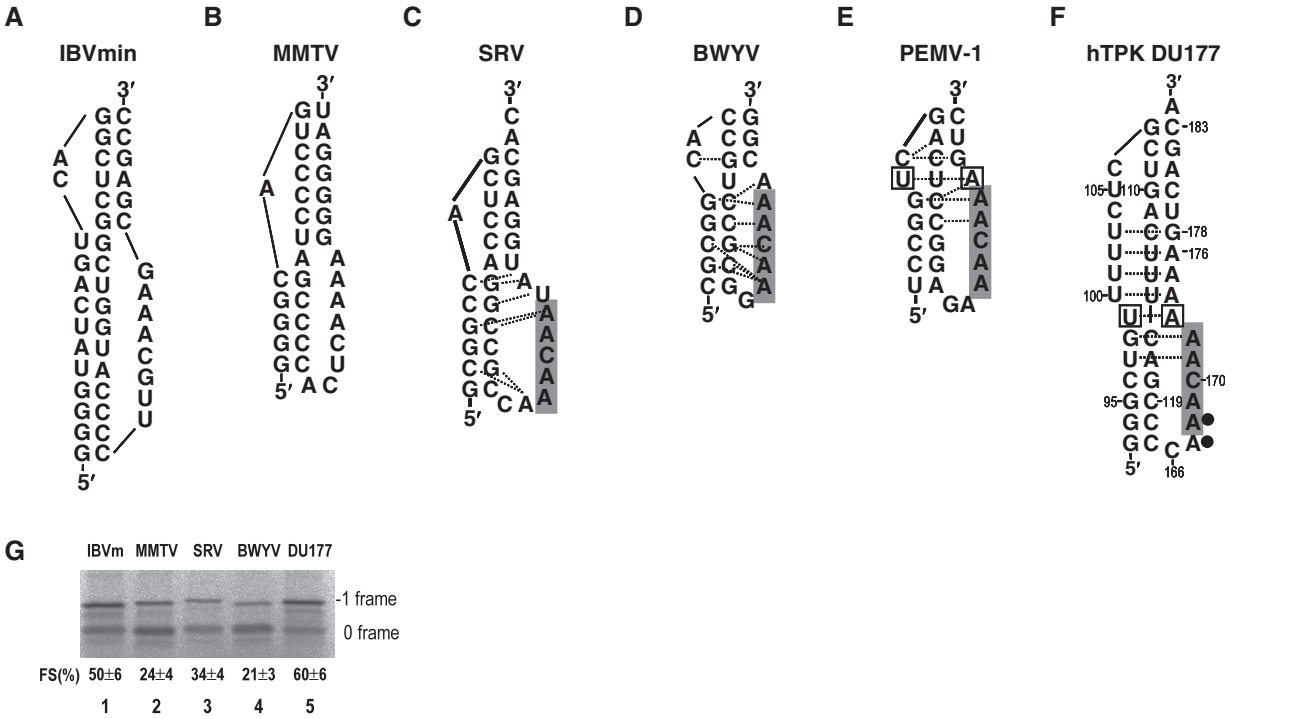

Figure 1. Sequence, secondary structure and tertiary interaction comparisons among DU177 and several −1 PRF pseudoknots. (**A**) IBVm-PK (24). (**B**) MMTV-PK (12). (**C**) SRV-PK (25). (**D**) BWYV-PK (22). (**E**) Pea enation mosaic virus RNA1 pseudoknot (PEMV-1 PK) (26). (**F**) DU177 RNA pseudoknot (33). The nucleotides in DU177 are numbered according to those in ref. (33). The common AACAA sequences are highlighted by gray shadow, the unusual Hoogsteen AU base pairs are boxed, and the adenines stacking and tertiary interactions are represented by filled circles and dotted lines, respectively. (**G**) The 12% SDS–PAGE analysis of the −1 PRF assays of several viral RNA pseudoknots, including a minimum IBV-PK (IBV_m-PK), MMTV-PK, SRV-PK, BWYV-PK and DU177 RNA (22,25,29,32,33). Each pseudoknot was incorporated into a pRL-SV40-based reporter, assayed as described in the 'Materials and Methods', and the translated proteins corresponding to the 0-frame and −1 frame products were labeled as indicated. Please note that a negative control without insertion of a pseudoknot only showed background −1 PRF activity (data not shown).

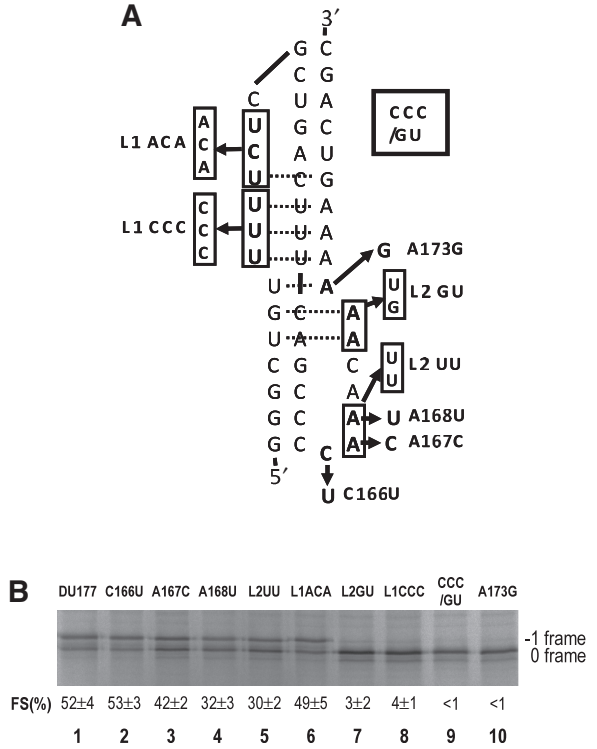

Figure 2. Both major- and minor-groove triple interactions in DU177 are required for efficient −1 PRF. (**A**) Illustration of mutagenesis scheme for the mutations in loops 1 and 2 of DU177. For each mutant, the nucleotide identities before and after mutation are typed in bold, linked by an arrow and labeled. In addition, mutants with multiple mutations are boxed. (**B**) The 12% SDS–PAGE analysis of −1 PRF assays of different loop mutation constructs. Individual mutant is indicated on top of the gel, with the translated proteins corresponding to the 0-frame and −1-frame products labeled as indicated. The calculated frameshift efficiencies (with standard deviation) are listed at the bottom of the gel and are the average of at least three repeated experiments. Please note that a p2luc reporter, with a stop codon inserted into the −1 frame of the N-terminal region of firefly luciferase, was used in these experiments and will thus generate a premature −1 frame protein product.

make it a good model molecule for dissecting the structural determinants within a pseudoknot for the stimulation of −1 PRF.

A structural feature found in several −1 PRF pseudoknot stimulators, which involved stacking of the loop 2 adenines in the minor groove of stem 1 in a pseudoknot, was also identified in DU177 (33). The residues 166–168 of DU177 were thus mutated, and the resulting mutants (C166U, A167C, A168U and L2-UU in Figure 2A) still possessed substantial −1 PRF activities ranging from 50% to 30% (Figure 2B, lanes 2–5). Similarly, mutagenesis on loop 1 nucleotides 103 and 105 generated mutant L1-ACA with a DU177-like −1 PRF activity (compare lane 1 with lane 6 in Figure 2B). Therefore, the −1 PRF activity of DU177 is not very sensitive to nucleotide identity in the 3′ portion of its loop 1.

As base–triple interactions were shown to be important for −1 PRF activity in several pseudoknots (22,25–28,32), we disrupted the three major-groove triples and the two minor-groove triples by making mutations on loops 1 and 2 of DU177, respectively. As shown in Figure 2B (lanes 7–9), the −1 PRF efficiencies of both mutants (L1-CCC and L2-GU) were reduced dramatically to below 5%, whereas the CCC/GU mutant, with all five base triples impaired, lost its −1 PRF activity to essentially 0%. The A173G mutant was then made to destroy the crucial Hoogsteen AU base pair that helps in anchoring the interhelical triplex. Similar to what was observed in CCC/GU mutant, this single mutation wiped out −1 PRF activity completely (Figure 2B, lane 10) and is consistent with the involvement of triplex formation in the stimulation of −1 PRF activity of DU177.

The DU177 and CCC/GU RNAs both adopt pseudoknot conformation

To examine if the mutants with disrupted base–triple interactions still adopt the pseudoknot conformation, non-denatured gel electrophoresis and enzymatic structure probing experiments were performed on CCC/GU RNA, and the results were compared with those of DU177 pseudoknot. Analysis of non-denatured gel confirmed that both RNA constructs adopt a major conformation (Figure 3A). However, distinct gel mobility of these two RNAs suggested that they might have different conformations. The enzymatic probing data are shown and summarized in Figure 3B–E. We used DU177 RNA as the standard for comparison because its NMR structure is well defined (33). For both DU177 and CCC/GU RNAs, the distributions of cleavage patterns by ribonuclease T2, the probe for single-stranded region, are in agreement with the formation of the two loop regions. In addition, the distributions of cleavage patterns by RNase V1, the probe for duplex and stacked conformations, can be localized to the two predicted stem regions for both RNAs. Specifically, both RNAs possess signature V1 cleavage for the quasi-continuous helical region corresponding to the 3′-portion of stem 1 and the 5′-portion of stem 2 (Figure 3B,D). Therefore, these probing data indicate that CCC/GU RNA also adopts a pseudoknot conformation and suggest that the other mutants containing more base triples should also adopt the pseudoknot conformations. In the related UV-melting and single-molecule mechanical unfolding experiments for DU177 and CCC/GU RNAs, transitions corresponding to the melting or mechanical unfolding of stems 1 and 2 were also observed and are consistent with the probing data (33,38). In addition, an extra transition corresponding to the disruption of tertiary interaction network was also reported in single-molecule unfolding studies and can only be observed in DU177 RNA (38). Taken together with the mutagenesis studies above, the results of these experiments suggest that DU177 RNA can be converted into a −1 PRF-incompetent pseudoknot by disruption of the triplex structure spanning the helical junction.

Stem–loop interactions and their relative position to the helical junction of pseudoknot affect the −1 PRF efficiency of DU177

To dissect the contribution of individual base–triple interaction in −1 PRF activity of DU177, we generated mutations in loops 1 and 2 to disrupt specific stem–loop

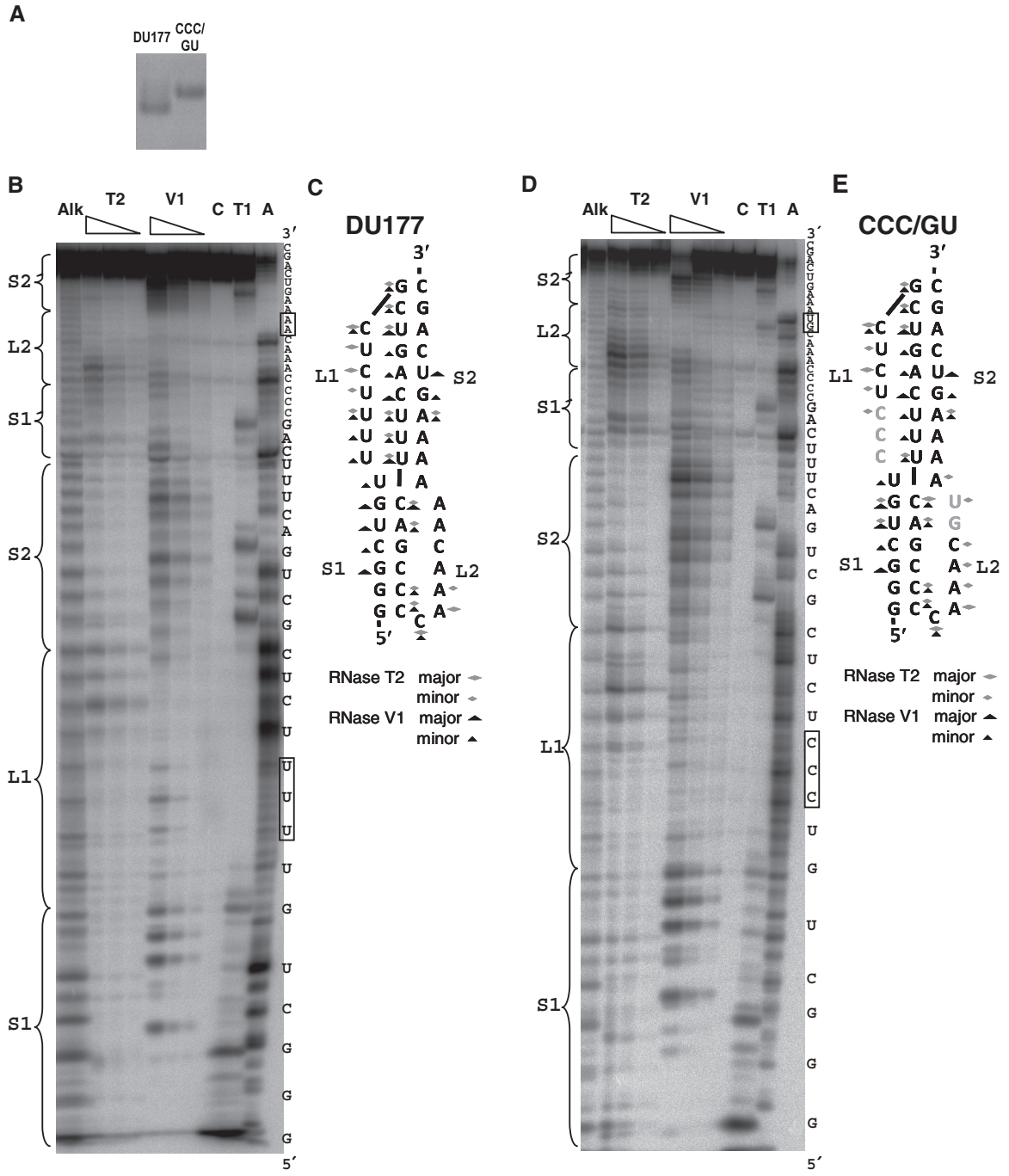

Figure 3. CCC/GU RNA adopts the conformation of a pseudoknot. (**A**) Gel-mobility assay results for DU177 and CCC/GU RNA analyzed by 20% native gel. (**B**) Electrophoretic analysis of the enzymatic probing data of DU177. (**C**) Summary of the cleavage patterns for DU177. (**D**) Electrophoretic analysis of the enzymatic probing data of CCC/GU RNA. (**E**) Summary of the cleavage patterns for CCC/GU RNA. The enzymatic cleavage results were resolved in a 20% sequencing gel, with the first and eighth wells as alkaline hydrolysis ladder and control, respectively, whereas the last two wells represent guanine and pyrimidine assignment markers. The cleavage results after RNase T2 and V1 treatments, with increment of RNase concentration, are shown in wells 2–4 and 5–7, respectively. In addition, the assigned residues and the corresponding stem/loop regions are listed on the right and left sides of the gel, respectively. Please note that the residues different from each other are boxed for comparison between both RNAs. Finally, the extent of cleavage for each probe is defined as major or minor cut, and summarized in (B) and (D), with gray rhombuses representing RNase T2 cleavage and filled triangles representing RNase V1 cleavage. They are presented along the predicted secondary structures of both RNAs, with the five mutated loop nucleotides in CCC/GU RNA typed in gray.

interactions (see Figure 4A for mutation scheme). As shown in Figure 4B, a dramatic reduction of −1 PRF activity to ∼10% can be observed for mutants U100C, U101C, A171G and A172U, whereas mutant U102C possesses a −1 PRF efficiency of 33% (Figure 4B, lanes 1–5). Therefore, the stem–loop interactions flanking the helical junction, contributed by the first two base triples of both stems, are crucial for efficient

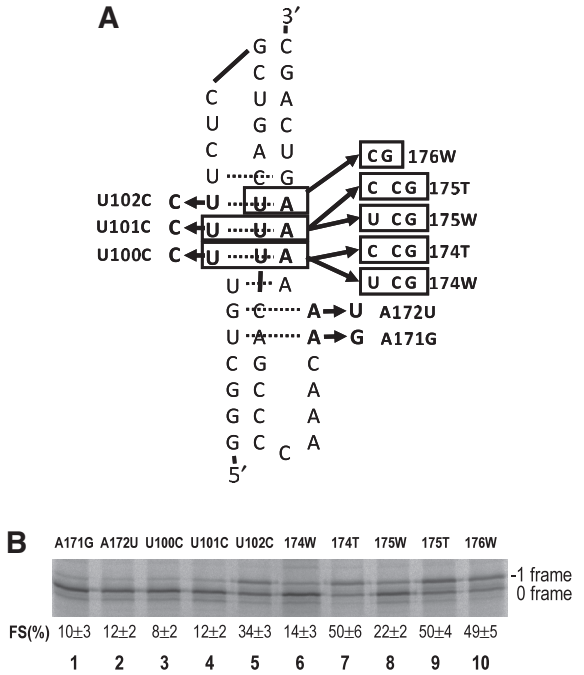

Figure 4. The −1 PRF assays for the stem–loop interaction dissection mutants of DU177. (**A**) Illustration of mutagenesis scheme for the mutations dissecting specific base–triple interactions. The mutants are designated as those in Figure 2A. (**B**) The 12% SDS–PAGE analysis of −1 PRF assays of different base–triple disruption mutants. Individual mutant is indicated on top of the gel, with the translated proteins corresponding to the 0-frame and −1-frame products labeled as indicated. The reporter construct is the same as Figure 2B, and the calculated −1 PRF efficiencies (with standard deviation) are listed at the bottom of the gel and are the average of at least three repeated experiments.

−1 PRF activity. In contrast, the stem–loop interactions from the distal third major-groove triple (U113-A176·U102) are less important. During the progress of this work, an extra major-groove base–triple was proposed in the refined DU177 structure (34). It locates next to the distal third triple, and its formation will be blocked in the L1-ACA mutant created in Figure 2. Both DU177 and L1-ACA having similar −1PRF efficiencies (compare lane 1 with lane 6 in Figure 2B) further support the idea that the contribution of a major-groove triple in −1 PRF activity of DU177 also depends on its relative position to the helical junction.

We further mutated the stem U-A base pair to the C-G base pair for every U-A·U major-groove triple (mutants 174W, 175W and 176W in Figure 4A). As shown in Figure 4B, each of these mutants possesses lower −1 PRF activity than that of DU177 (Figure 4B, lanes 6, 8 and 10). The frameshift activities range from 49% for 176W to 22 and 14% for 175W and 174W, respectively. Therefore, mutation on the stem base pair of the distal third major-groove triple, 176W, has less impact on −1 PRF activity than those of the two junction-flanking major-groove triples. Finally, mutating the U of C–G · U triple (174W or 175W) to the C, thus forming a C–G · C triple (174T or 175T), can restore frameshift efficiency to the level of DU177. Interestingly, the U–A · U triple, with a weaker U–A base pair in the stem, seems to have higher −1 PRF activity than the C–G · U base–triple containing a stronger stem C–G base pair. Taken together, these data strongly suggest that the stem–loop interactions in the major-groove triples and their positions relative to the helical junction play important roles in the −1 PRF activity of DU177.

A triplex formed intermolecularly to mimic triplex structure in DU177 can stimulate −1 PRF

Previous studies have shown that the tertiary interactions in human telomerase RNA pseudoknot region can be maintained in a two-piece assembly (35). Indeed, UV-melting experiments on a bimolecular pseudoknot have indicated that the triplex formation is independent of loop closure embedded in the pseudoknot topology (33). Because of the dominant role of triplex formation in the −1 PRF activity of DU177 revealed above, we used a similar bimolecular pesudoknot approach to examine the contribution of pseudoknot topology to the −1 PRF activity of DU177. In this approach, the 5′-hairpin portion of DU177 was used to replace the DU177 pseudoknot in the reporter mRNA to form the hTR-5′hp construct, and an in-trans hTR3′ss RNA corresponding to the loop 2 and the 3′ portion of stem 2 in DU177 was constructed separately (Figure 5A). Based on the results from previous UV-melting experiments (33), the association of hTR3′ss RNA with hTR–5′hp construct will restore stem 2 and all the triple interactions corresponding to those in the DU177. The bimolecular pseudoknot construct will thus resemble the unimolecular DU177, except for it missing the covalent linkage that connects stem 1 and loop 2. The results shown in Figure 5B indicate that, upon the addition of hTR3′ss RNA, the −1 PRF efficiency of 5′-hairpin-containing mRNA reporter (hTR-5′hp) changes from 0.25 to 5% in a dosage-dependent way. In contrast, a control mRNA reporter, hTR5′hp-L1c, designed to disrupt a potential intermolecular major-groove base–triple interactions, does not respond to even a higher dosage of hTR3′ss RNA. Similarly, in-*trans* oligo-nucleotides (171G3′ss and 172U3′ss RNA), designed to disrupt potential intermolecular minor-groove base–triple interactions, cannot induce significant −1 PRF activity on hTR5′hp mRNA reporter, either (Figure 5C). Finally, we also examined if an intermolecular U–A · U major-groove base–triple interaction can be replaced by an intermolecular C–G · C triple. As shown in Figure 6, 174T3′ss RNA, designed to form a C–G · C triple with 174T5′hp mRNA reporter, can stimulate significant −1 PRF activity on 174T5′hp reporter only, but not on hTR5′hp or hTR5′hp-L1c reporter. Therefore, an intermolecular triplex mimicking the triplex structure spanning the helical junction of DU177, although it does not possess a completed pseudoknot topology, can stimulate −1 PRF activity. Together with the observation that the removal of the continuing triplex structure converts DU177 into a −1 PRF incompetent pseudoknot, these experimental results argue that both the pseudoknot topology and the triplex structure are required for high-efficiency of −1 PRF, with the

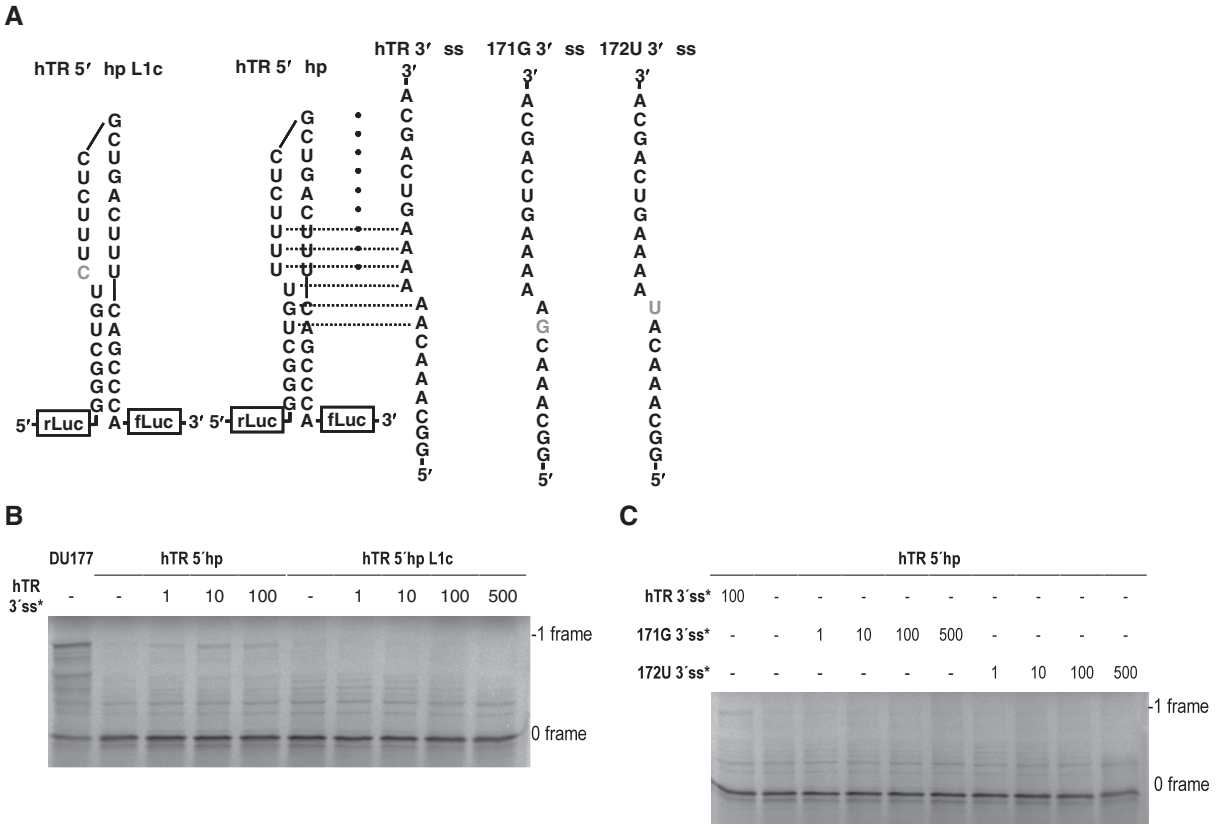

Figure 5. DU177-mimicking intermolecular triplex can act as a stimulator of −1 PRF. (**A**) Schematic explanation for constructs used in the biomolecular pseudoknot approach. The base pairs formed intermolecularly are represented by filled circles, whereas tertiary base–triple interactions are shown by dotted lines. The nucleotides that will interfere with base triple formation in the bimolecular construct are typed in gray. Please note that the slippery site and spacer are not shown in the drawing, and a p2luc reporter, with a full-length firefly luciferase generated as the −1 frame product, was used in this experiment. (**B**) Results of −1 PRF assays of intermolecular major-groove base triple analysis. (**C**) Results of −1 PRF assays of intermolecular minor-groove base triple analysis. The designated asterisk indicates the estimated molecular ratios between the in-trans RNA (hTR3′ss, 171G3′ss and 172U3′ss) and the mRNA reporter (hTR5′hp and hTR5′hpL1c), and the translated proteins corresponding to the 0-frame and −1 frame products are also labeled.

pseudoknot topology playing an enhancer-like role to further increase −1 PRF efficiency.

DISCUSSION

Dissection of base–triple interactions and effect of stem–loop interactions on −1 PRF activity of DU177

Mutational analysis indicate that mutants with junction-flanking C–G·U or C–G·C triple do not have higher −1 PRF activity than those of DU177 with U–A·U triple occupying the same position. This is intriguing as one extra hydrogen bond is contributed by the stem C–G base pairing in the process of the U–A·U to C–G·U conversion. However, one stem–loop interbase hydrogen bond is also lost at the same time. In contrast to the C–G·U triple, the C–G·C triple can possess more than one Hoogsteen interaction depending on the pH condition (39), and the −1 PRF efficiency may thus be restored to the level of U–A·U triple. Therefore, it suggests the important role of tertiary stem–loop interactions in modulating the −1 PRF activity of DU177.

Role of junction-proximal stem–loop interaction in the modulation of frameshift efficiency

As demonstrated by the observation that disruption of the adenine stacking between loop 2 and stem 1 of DU177 also affects the −1 PRF efficiency of DU177, there may be more than one way to interfere with the helicase activity of a translocating ribosome. The studies on −1 PRF pseudoknots containing short stem 1, such as BWYV-PK and ScYLV-PK, indicated that specific minor-groove base triples involving S1 and L2 are important for −1 PRF activity, and the impact on frameshift efficiency depends on their relative position to the helical junction (27,28,30,31). Particularly, it has been shown that junction-flanking tertiary interactions between the 3′-nucleotide of loop 2 and base pairing in stem 1 can organize an interhelical interaction network that may act as a kinetic barrier during the unfolding of pseudoknot by ribosome (28). In contrast, the roles of loop 1 and stem 2 in a −1 PRF pseudoknot stimulator are less addressed as both BWYV-PK and ScYLV-PK have short loop 1 and stem 2 (18). In this work, we reveal that the major-groove

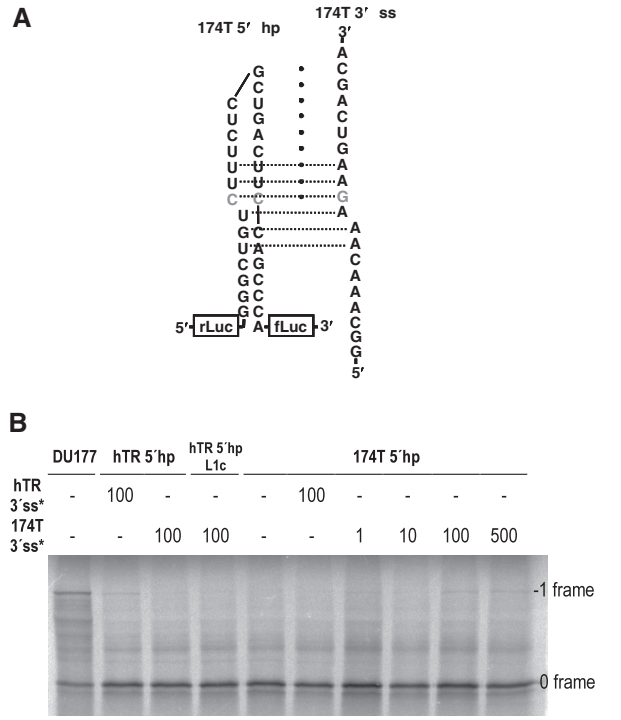

Figure 6. An intermolecular C-GC major-groove base–triple interaction can replace an intermolecular U-AU triple. The C-G·C major-groove base–triple interaction reconstituted in the bimolecular pseudoknot construct is typed in gray, and the other designations are the same as those in Figure 5.

base–triple interactions closer to the helical junction are more important than the distal ones for −1 PRF activity of DU177 (Figures 2B and 4B). Therefore, the relative position toward the helical junction is important for both major- and minor-groove base–triple in determining the contribution of a base–triple to the −1 PRF stimulation activity of a pseudoknot. This position-dependent effect can be rationalized by the stabilization of stem 2 by stem–loop interactions, and the anchoring of stem 2 into stem 1 via the junction bridging triplex formation. Such interactions will provide extra restraints during the unwinding of stem 1 by ribosome and are consistent with the torsional restraint hypothesis (18).

Both the helical geometry of a pseudoknot and its ability to against deformation by a ribosome can be affected by the stem–loop interaction in a position-dependent way, too. Indeed, modulation of frameshift efficiency by the modification of junction geometry via tertiary interactions has been observed in the helical junction of MMTV-PK and BWYV-PK (29,30). In particular, the DU177 pseudoknot also adopts a bent conformation around the helical junction (33,34), and the tertiary stem–loop interactions contributed by the junction-flanking base triples may thus play a unique role to facilitate this bending process. Alternatively, the single-molecule unfolding analysis of a set of DU177 variants, with −1 PRF efficiency ranging from 50 to 0%, reveals a correlation between pseudoknot mechanical stability and frameshift efficiency (38). Building upon this foundation, the position effect of stem–loop interaction on the mechanical stability of a pseudoknot can be analyzed further in the future.

The roles of loop-closure constraint within a −1 PRF pseudoknot stimulator

The stimulation of −1 PRF activity by a bimolecular pseudoknot mimicking DU177 suggests an enhancement role for the pseudoknot topology in −1 PRF activity, particularly for those pseudoknots possessing a short stem 1 (22,25–28,32). In these cases, the pseudoknot topology may just serve to hold the structural determinants of −1 PRF activity together within the same molecule. With loops crossing the grooves of stems under the pseudoknot topology, an interlocked helical junction can be efficiently generated by the junction-flanking stem–loop interactions, and thus restrict the rotational flexibility between stems 2 and 1 as proposed in the torsional restraint hypothesis (18). In addition, the loop 2 to stem 1 adenine stacking interactions described above can be put in place easily. Alternatively, the fact that most −1 PRF competent pseudoknots possess a short loop 1, thus creating strains (40), argues for a more active role for the loop-closure constraint imposed by a pseudoknot. In fact, the bimolecular pseudoknot construct still maintains one of the two constrained loops seen in DU177, and the intact DU177 indeed has a much higher −1 PRF efficiency than that of the bimolecular pseudoknot. This can explain why removing one loop-closure constraint from DU177 can reduce its −1 PRF efficiency dramatically, and thus underscores the importance of pseudoknot topology in −1 PRF. In agreement with this work, designed RNA–DNA hybrids, with loop–loop interaction between mRNA and in-trans DNA hairpin to mimick rotational restraints imposed by pseudoknot topology, have been shown to stimulate −1 PRF significantly (18).

Telomerase, −1 PRF and applications of bimolecular pseudoknot

It is intriguing that an RNA motif derived from the RNA component of telomerase can act as a −1 PRF stimulator. This could be explained by the existence of a common structural feature such as a specific RNA-protein contact, which is needed for a telomerase as well as a −1 PRF stimulator to function properly. Interestingly, telomerase RNA subunit has been identified in Marek's disease virus (41). Perhaps, different viruses might pick up this motif during evolution and modified it to fit replication purpose, including the tuning of −1 PRF efficiency through mutation (30). Nevertheless, it is informative to note that specific 2′OH groups protruding from the triple helix of DU177 have been shown to contact with the protein component of telomerase (42). Therefore, the bimolecular pseudoknot provides a workable platform to explore the possibility of specific stimulator-ribosomal helicase interaction during −1 PRF as suggested previously (22). In addition, it should be useful in probing the geometry of the mRNA entry channel and the helicase activity of eukaryotic ribosomes. Finally, the regulation of −1 PRF in-*trans* shown here raises the possibility that

non-coding RNA may use a similar mechanism to regulate gene expression although the −1 PRF efficiency observed here is not dramatic compared with the reported examples (20,21). However, further enhancement of frameshift efficiency for application purpose is possible, such as that demonstrated by the use of modified oligonucleotides (20).

ACKNOWLEDGEMENTS

The authors thank Mr Che-Pei Chuo for technical assistance, Dr John Atkins for plasmid p2Luc, and Professor Nacho Tinoco and Dr Gang Chen for their useful discussion and reading of the manuscript.

FUNDING

Grant NSC 95-2311-B-005-013 from the National Science Council of Taiwan (to K.-Y.C). Funding for open access charge: National Chung-Hsing University, Taiwan.

Conflict of interest statement. None declared.

REFERENCES

1. Farabaugh,P.J. (1996) Programmed translational frameshifting. *Microbiol. Rev.*, **60**, 103–134.
2. Gesteland,R.F. and Atkins,J.F. (1996) Recoding: dynamic reprogramming of translation. *Annu. Rev. Biochem.*, **65**, 741–768.
3. Jacks,T. and Varmus,H.E. (1985) Expression of the Rous sarcoma virus polgene by ribosomal frameshifting. *Science*, **230**, 1237–1242.
4. Jacks,T., Madhani,H.D., Masiarz,F.R. and Varmus,H.E. (1988) Signals forribosomal frameshifting in the Rous sarcoma virus gag-pol region. *Cell*, **55**, 447–458.
5. Jacks,T., Power,M.D., Masiarz,F.R., Luciw,P.A., Barr,P.J. and Varmus,H.E. (1988) Characterization of ribosomal frameshifting in HIV-1 gag-pol expression. *Nature*, **331**, 280–283.
6. Brierley,I., Digard,P. and Inglis,S.C. (1989) Characterization of an efficient coronavirus ribosomal frameshifting signal: requirement for an RNA pseudoknot. *Cell*, **57**, 537–547.
7. Dinman,J.D., Icho,T. and Wickner,R.B. (1991) A −1 ribosomal frameshift in a double-stranded RNA virus of yeast forms a gag-pol fusion protein. *Proc. Natl Acad. Sci. USA*, **88**, 174–178.
8. Manktelow,E., Shigemoto,K. and Brierley,I. (2005) Characterization of the frameshift signal of Edr, a mammalian example of programmed −1 ribosomal frameshifting. *Nucleic Acids Res.*, **33**, 1553–1563.
9. Wills,N.M., Moore,B., Hammer,A., Gesteland,R.F. and Atkins,J.F. (2006) A functional −1 ribosomal frameshift signal in the human paraneoplastic Ma3 gene. *J. Biol. Chem.*, **281**, 7082–7088.
10. Jacobs,J.L., Belew,A.T., Rakauskaite,R. and Dinman,J.D. (2007) Identification of functional, endogennous programmed −1 ribosomal frameshift signals in the genome of *Saccharomyces cerevisiae*. *Nucleic Acids Res.*, **35**, 165–174.
11. Brierley,I., Jenner,A.J. and Inglis,S.C. (1992) Mutational analysis of the 'slippery-sequence' component of a coronavirus ribosomal frameshifting signal. *J. Mol. Biol.*, **227**, 463–479.
12. Chamorro,M., Parkin,N. and Varmus,H.E. (1992) An RNA pseudoknot and an optimal heptameric shift site are required for highly efficient ribosomal frameshifting on a retroviral messenger RNA. *Proc. Natl Acad. Sci. USA*, **89**, 713–717.
13. Yusupova,G.Z., Yusupov,M.M., Cate,J.H. and Noller,H.F. (2001) The path of messenger RNA through the ribosome. *Cell*, **106**, 233–241.
14. Takyar,S., Hickerson,R.P. and Noller,H.F. (2005) mRNA helicase activity of the ribosome. *Cell*, **120**, 49–58.
15. Plant,E.P., Jacobs,K.L., Harger,J.W., Meskauskas,A., Jacobs,J.L., Baxter,J.L., Petrov,A.N. and Dinman,J.D. (2003) The 9-A solution: how mRNA pseudoknots promote efficient programmed −1 ribosomal frameshifting. *RNA*, **9**, 168–174.
16. Giedroc,D.P., Theimer,C.A. and Nixon,P.L. (2000) Structure, stability and function of RNA pseudoknots involved in stimulating ribosomal frameshifting. *J. Mol. Biol.*, **298**, 167–185.
17. Tu,C., Tzeng,T.-H. and Bruenn,J.A. (1992) Ribosomal movement impeded at a pseudoknot required for frameshifting. *Proc. Natl Acad. Sci. USA*, **89**, 8636–8640.
18. Plant,E.P. and Dinman,J.D. (2005) Torsional restraint: a new twist on frameshifting pseudoknots. *Nucleic Acids Res.*, **33**, 1825–1833.
19. Dulude,D., Baril,M. and Brakier-Gingras,L. (2002) Characterization of the frameshift stimulatory signal controlling a programmed −1 ribosomal frameshift in the human immunodeficiency virus type 1. *Nucleic Acids Res.*, **30**, 5094–5102.
20. Howard,M.T., Gesteland,R.F. and Atkins,J.F. (2004) Efficient stimulation of site-specific ribosome frameshifting by antisense oligonucleotides. *RNA*, **10**, 1653–1661.
21. Olsthoorn,R.C.L., Laurs,M., Sohet,F., Hilbers,C.W., Heus,H.A. and Pleij,C.W.A. (2004) Efficient stimulation of site-specific ribosome frameshifting by antisense oligonucleotides. *RNA*, **10**, 1702–1703.
22. Su,L., Chen,L., Egli,M., Berger,J.M. and Rich,A. (1999) Minor groove RNA triplex in the crystal structure of a ribosomal frameshifting viral pseudoknot. *Nat. Struct. Biol.*, **6**, 285–292.
23. Chen,X., Kang,H., Shen,L.X., Chamorro,M., Varmus,H.E. and Tinoco,I. Jr (1996) A characteristic bent conformation of RNA pseudoknots promotes −1 frameshifting during translation of retroviral RNA. *J. Mol. Biol.*, **260**, 479–483.
24. Napthine,S., Liphardt,J., Bloys,A., Routledge,S. and Brierley,I. (1999) The role of RNA pseudoknot stem 1 length in the promotion of efficient −1 ribosomal frameshifting. *J. Mol. Biol.*, **288**, 305–320.
25. Michiels,P.J.A., Versleijen,A.A.M., Verlaan,P.W., Pleij,C.W.A., Hilbers,C.W. and Heus,H.A. (2001) Solution structure of the pseudoknot of SRV-1 RNA, involved in ribosomal frameshifting. *J. Mol. Biol.*, **310**, 1109–1123.
26. Nixon,P.L., Rangan,A., Kim,Y.G., Rich,A., Hoffman,D.W., Hennig,M. and Giedroc,D.P. (2002) Solution structure of a luteoviral P1-P2 frameshifting mRNA pseudoknot. *J. Mol. Biol.*, **322**, 621–633.
27. Cornish,P.V., Henning,M. and Giedroc,D.P. (2005) A loop 2 cytidine–stem 1 minor groove interaction as a positive determinant for pseudoknot-stimulated −1 ribosomal frameshifting. *Proc. Natl Acad. Sci. USA*, **96**, 12694–12699.
28. Cornish,P.V., Stammler,S.N. and Giedroc,D.P. (2006) The global structures of a wild-type and poorly functional plant luteoviral mRNA pseudoknot are essentially identical. *RNA*, **12**, 1959–1969.
29. Chen,X., Chamorro,M., Lee,S.I., Shen,L.X., Hines,J.V., Tinoco,I. Jr and Varmus,H.E. (1995) Structural and functional studies of retroviral RNA pseudoknots involved in ribosomal frameshifting: nucleotides at the junction of the two stems are important for efficient ribosomal frameshifting. *EMBO J.*, **14**, 842–852.
30. Kim,Y.G., Su,L., Maas,S., O'Neill,A. and Rich,A. (1999) Specific mutations in a viral RNA pseudoknot drastically change ribosomal frameshifting efficiency. *Proc. Natl Acad. Sci. USA*, **96**, 14234–14239.
31. Kim,Y.G., Naas,S., Wang,S.C. and Rich,A. (2000) Mutatioal study reveals that tertiary interactions are conserved in in ribosomal frameshifting pseudoknot of two luteoviruses. *RNA*, **6**, 1157–1165.
32. Liphardt,J., Napthine,S., Kontos,H. and Brierley,I. (1999) Evidence for an RNA pseudoknot loop-helix interaction essential for efficient −1 ribosomal frameshifting. *J. Mol. Biol.*, **288**, 321–335.
33. Theimer,C.A., Blois,C.A. and Feigon,J. (2005) Structure of the human telomerase RNA pseudoknot reveals conserved tertiary interactions essential for function. *Mol. Cell.*, **17**, 671–682.
34. Kim,N.K., Zhang,Q., Zhou,J., Theimer,C.A., Peterson,R.D. and Feigon,J. (2008) Solution structure and dynamics of the wild-type

pseudoknot of human telomerase RNA. *J. Mol. Biol.*, **384**, 1249–1261.
35. Chen,J.-L. and Greider,C.W. (2005) Functional analysis of the pseudoknot structure in human telomerase RNA. *Proc. Natl Acad. Sci. USA*, **102**, 8080–8085.
36. Grentzmann,G., Ingram,J.A., Kelly,P.J., Gesteland,R.F. and Atkins,J.F. (1998) A dual-luciferase reporter system for studying recoding signals. *RNA*, **4**, 479–486.
37. Su,M.C., Chang,C.T., Chu,C.H., Tsai,C.H. and Chang,K.Y. (2005) An atypical RNA pseudoknot stimulator and an upstream attenuation signal for −1 ribosomal frameshifting of SARS coronavirus. *Nucleic Acids Res.*, **33**, 4265–4275.
38. Chen,G., Chang,K.-Y., Chou,M.-Y., Bustamante,C. and Tinoco,I. Jr (2009) Triplex structures in an RNA pseudoknot enhance mechanical stability and increase efficiency of −1 ribosomal frameshifting. *Proc. Natl Acad. Sci USA*, **106**, 12706–12711.
39. Soto,A.M., Loo,J. and Marky,L.A. (2002) Energetic contributions for the formation of TAT/TAT, TAT/CGC^+, and CGC^+/CGC^+ base triplet stacks. *J. Am. Chem. Soc.*, **124**, 14355–14363.
40. Wyatt,J.R., Puglisi,J.D. and Tinoco,I. Jr (1990) RNA pseudoknots: stability and loop size requirements. *J. Mol. Biol.*, **214**, 455–470.
41. Fragnet,L., Blasco,M., Klapper,W. and Rasschaert,D. (2003) The RNA subunit of telomerase is encoded by Marek's disease virus. *J. Virol.*, **77**, 5985–5996.
42. Qiao,F. and Cech,T.R. (2008) Triple-helix structure in telomerase RNA contributes to catalysis. *Nat. Struct. Mol. Biol.*, **15**, 634–640.